



Advancing the Modeling, Understanding, and Prediction of Weather and Climate

POSSIBLE ANTHROPOGENIC ENHANCEMENT OF PRECIPITATION IN THE SAHEL-SUDAN SAVANNA BY REMOTE AGRICULTURAL IRRIGATION

Geophysical Research Letters Y. Zeng¹, P.C.D. Milly², E. Shevliakova³, S. Malyshev³, M. van Huijgevoort¹, K.A. Dunne⁴

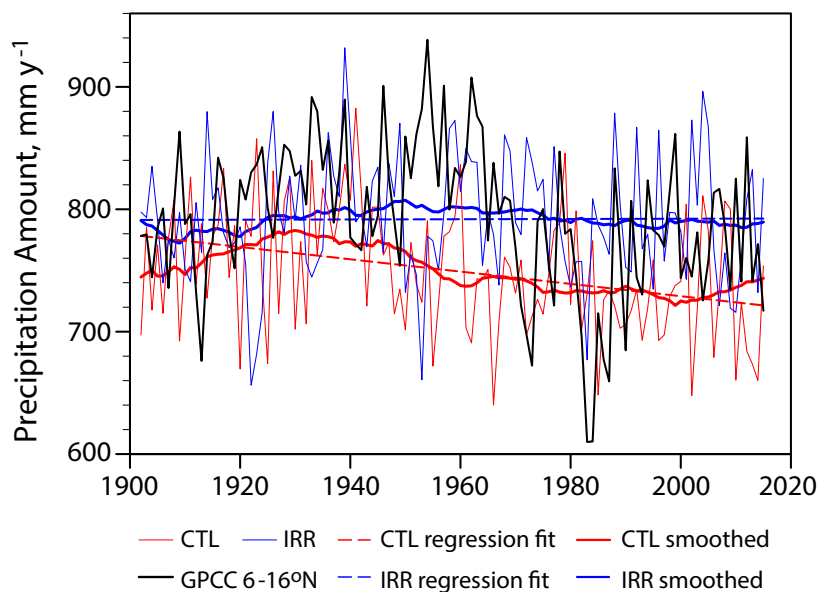
DOI: [10.1029/2021GL096972](https://doi.org/10.1029/2021GL096972)

The goal of this research was to identify remote climatic impacts of global irrigation. From the start of the 20th century, the global area equipped for irrigation grew several-fold to encompass 1.8% of the global land area by the year 2015. Recently, climate models have begun to yield a picture of the resultant global impacts on historical climate. Local effects on surface water and energy budgets are profound and robust, but the impacts on precipitation, particularly those far from irrigated regions, are model-dependent and uncertain, and their governing mechanisms generally have not been analyzed in depth.

The authors performed historical climate experiments with a GFDL Earth system model, with and without modification to account for global irrigation. **Results show that the enhancement of Sahel precipitation by irrigation in the Middle East and the Indian sub-continent is approximately equal and opposite to the reduction of precipitation induced by the combination of all previously considered natural and anthropogenic factors.**

Interestingly, the enhancement mechanism does not involve increased transport of moisture from the irrigated regions to the region of precipitation enhancement. Rather, the irrigation-induced increase of moist static energy, upon transport to the Sahel, destabilizes the atmosphere, causing an increase of precipitation, which is then amplified by positive feedbacks. Remote irrigation may have reduced the intensity of drought and famine in the 1970s-1980s, which appear to have been associated with anomalous ocean-surface temperatures. Future water availability in the Sahel may be affected by such factors as the depletion of groundwater resources in the Indian subcontinent and the pace of rehabilitation of irrigation infrastructure in the Middle East that was damaged by the Islamic State of Iraq and the Levant.

OAR Goals: [Detect Changes in the Ocean and Atmosphere](#); [Drive Innovative Science](#)



Impact of Middle East Irrigation on Sahel Precipitation

Model estimates of the forced component of the Sahel precipitation amount. Red curves (CTL) result from historical+RCP4.5 CMIP5 climate forcing; blue curves (IRR) result when irrigation is added to the standard CMIP5 climate forcing; black curves (GPC6-16°N) result from Global Precipitation Climatology Centre observations. Smoothed bold red (CTL smoothed) and blue (IRR smoothed) lines curve results from 30-year moving average without and with irrigation, respectively. Dashed red (CTL regression fit) and blue (IRR regression fit) lines curve results from linear regression fits to the simulated precipitation without and with irrigation forcing, respectively.

¹Program in Atmospheric and Oceanic Sciences, Princeton University, Princeton, NJ; ²U.S. Geological Survey, Princeton, NJ, USA; ³NOAA/GFDL, Princeton, NJ
⁴U.S. Geological Survey, Cornish, NH

PROSPECTS FOR SEASONAL PREDICTION OF SUMMERTIME TRANS-ARCTIC SEA ICE PATH

Journal of Climate M. Winton¹, M. Bushuk^{1,2}, Y. Zhang³, B. Hurlin¹, L. Jia^{1,2}, N. C. Johnson¹, F. Lu^{1,2}

DOI: [10.1175/JCLI-D-21-0634.1](https://doi.org/10.1175/JCLI-D-21-0634.1)

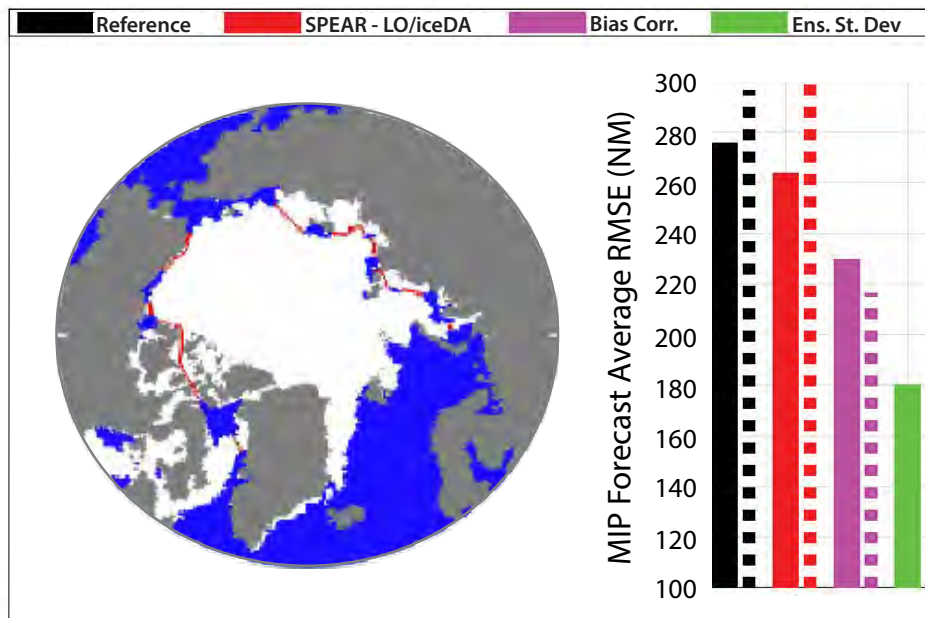
Northern Hemisphere sea ice cover has declined in recent decades, particularly in late summer when the ice edge retreats into the Arctic Ocean. This decline is well documented with satellite observations and is simulated by climate models as a response to anthropogenic forcing, indicating that the downward trend will continue into the future. The reduction in ice extent has led to ice-free corridors appearing in September in recent years. Seasonal prediction of the sea ice cover along these routes could support the increasing summertime ship traffic taking advantage of low ice conditions.

Using 1992-2017 retrospective predictions, this research demonstrates that the GFDL SPEAR forecast system produces skillful seasonal forecasts of summertime daily minimal Arctic sea ice path (MIP) between Atlantic and Pacific Oceans, corresponding roughly to the Northeast and Northwest Passages. However, the MIP forecast errors are generally similar to those of a damped persistence reference forecast.

The authors analyzed the forecast errors to identify potential skill improvements, finding large opportunities for forecast error reduction, especially at lead times of less than two months. Most of this potential improvement remains after linear removal of climatological and trend biases, suggesting significant error reduction might come from improved summertime thickness initialization and simulation of sub-annual variability. These findings indicate that current seasonal sea ice prediction systems can provide useful shipping-relevant information to users and that future systems have additional room for improvement.

OA Goals: [Make Forecasts Better](#); [Drive Innovative Science](#)

Skillful SPEAR Seasonal Forecasts of Summertime Daily Minimal Arctic Sea Ice Path



Left Example: Northwest and Northeast minimal sea ice paths (MIPs, red) calculated from the Arctic sea ice cover on 15 July 1992 (white).

Right: Statistical reference forecast error (black) compared to SPEAR before (red) and after (magenta) bias correction. Minimal error estimated as the forecast ensemble spread is shown in green. Dashed lines represent errors evaluated using sea ice cover observations derived using an alternative algorithm. The maximum potential error reduction corresponds to the difference between the red and green RMSEs.

¹NOAA/GFDL, Princeton, NJ; ²University Corporation for Atmospheric Research, Boulder, CO; ³Atmospheric and Oceanic Sciences Program, Princeton University, Princeton, NJ

A STUDY OF AR-, TS-, AND MCS-ASSOCIATED PRECIPITATION AND EXTREME PRECIPITATION IN PRESENT AND WARMER CLIMATES

Journal of Climate *Ming Zhao*¹

DOI: [10.1175/JCLI-D-21-0145.1](https://doi.org/10.1175/JCLI-D-21-0145.1)

Atmospheric rivers (AR), tropical storms (TS), and mesoscale convective systems (MCS) are important phenomena which often threaten society through heavy precipitation and strong winds. However, their roles in global mean and extreme precipitation have not been systematically explored. Using observational and reanalysis data and GFDL's new high-resolution atmospheric model (AM4 at 50km-resolution) this study shows for the first time that despite their occasional occurrence, taken together, AR, TS, and MCS days account for ~55% of global mean precipitation and ~75% of extreme precipitation with daily rates exceeding its 99th percentile.

Under a warmer climate, the changes in global mean and regional distribution of precipitation correspond well with the changes in AR/TS/MCS precipitation. Globally, the frequency of AR days increases slightly while the frequency of TS/MCS days decreases. The AR/TS/MCS mean precipitation intensity increases by ~5%/K, due primarily to precipitation increases in the top 25% of AR/TS/MCS days with the heaviest precipitation. These are dominated by the thermodynamic component, with the dynamic and microphysical components playing a secondary role.

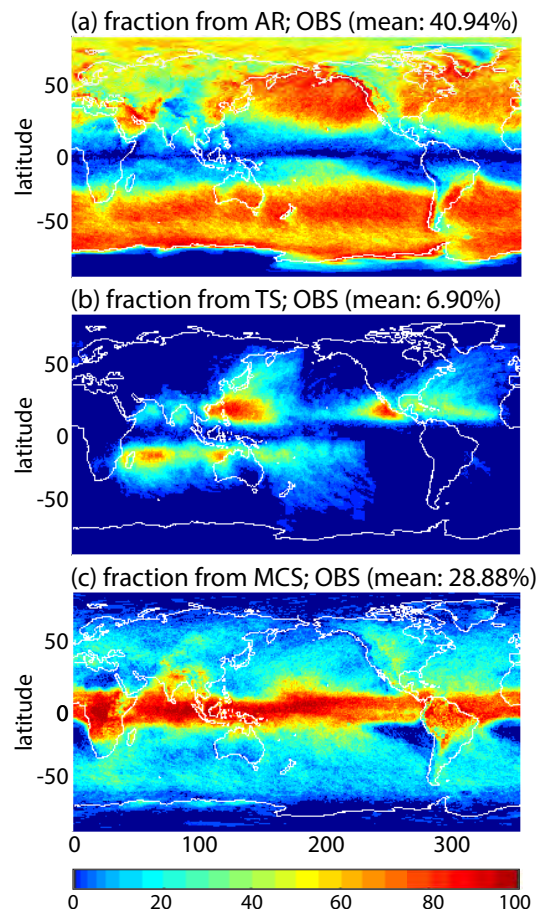
The frequency of AR days increases and migrates toward higher latitudes while the frequency of TS days increases over the central Pacific and part of the south Indian Ocean while decreasing elsewhere. The frequency of MCS days tends to increase over parts of the equatorial western and eastern Pacific warm pools and high latitudes and decreases over most parts of the tropics and subtropics.

This study offers a better understanding of the connections between extreme weather and the global and regional hydrological cycle in a changing climate, enhancing society's ability to plan and respond.

OAR Goals: Drive Innovative Science

¹NOAA/Geophysical Fluid Dynamics Laboratory, Princeton, NJ

Extreme Daily Precipitation Events from Atmospheric Rivers, Tropical Storms, and Mesoscale Convective Systems



Fraction (%) of the observed extreme daily precipitation events (defined as local 1% heaviest daily precipitation events) that come from the (top panel) atmospheric rivers (AR), (middle panel) tropical storms (TS), and (lower panel) mesoscale convective systems (MCS) days. See the model results in Figure 5 of the paper.

See GFDL's full bibliography at: <https://www.gfdl.noaa.gov/bibliography>

The bibliography contains professional papers by GFDL scientists and collaborators from 1965 to present day. You can search by text found in the document title or abstract, or browse by author, publication, or year.

IMPORTANT FACTORS IN THE TRACKING OF TROPICAL CYCLONES IN OPERATIONAL MODELS

Journal of Applied Meteorology and Climatology *T. Marchok*¹

DOI: [10.1175/JAMC-D-20-0175.1](https://doi.org/10.1175/JAMC-D-20-0175.1)

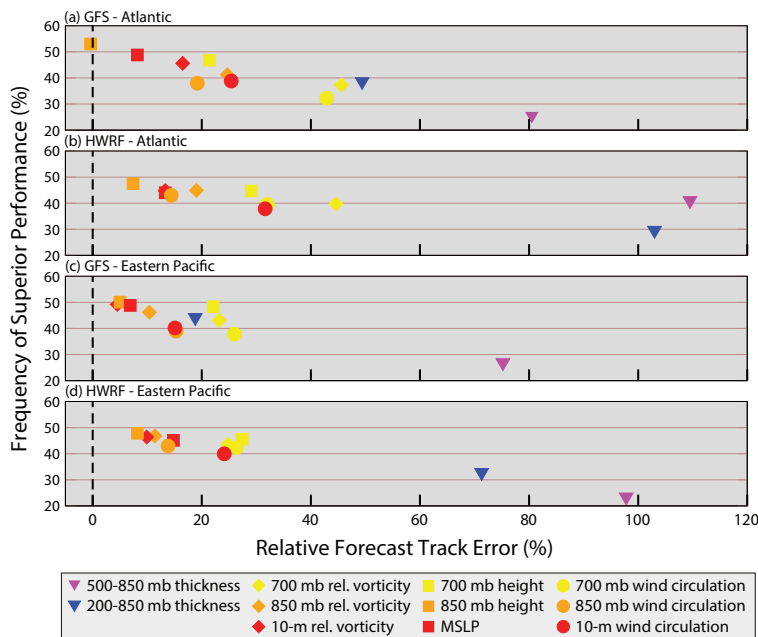
Providing model-based tropical cyclone (TC) track guidance to forecasters and emergency managers is a critical component of operational hurricane forecasting and is crucial for the protection of life and property. Track forecast errors, whether attributable to model or tracker issues, can have implications for a number of downstream applications, including the selection of areas to be included in watches and warnings. **The first study of its kind, this research provides an in-depth analysis into factors that can improve the accuracy and availability of that operational guidance.** Overall, tracker configurations composed of multiple variables are more reliable in providing guidance through the end of a forecast period than are tracker configurations based on individual parameters.

One of the key numerical weather prediction components in the operational forecast process for TCs is the use of an automated vortex tracker. A vortex tracking system provides an objective, automated method for scanning the digital output of a model and creating guidance for forecasters on metrics such as the predicted track, minimum sea-level pressure, maximum near-surface wind speed, and near-surface wind structure diagnostics for existing TCs.

Multiple configurations of the GFDL vortex tracker were tested, including numerous single-variable configurations, using two different operational models (Global Forecast System and Hurricane Weather Research and Forecast model) over a large number of cases from the 2015-2017 Atlantic and eastern Pacific hurricane seasons. Results revealed that a configuration composed of the mean of eleven tracking variables outperformed all individual configurations. Additionally, configurations composed of multiple variables are more reliable in tracking a cyclone to its completion in the model forecast and providing guidance through the end of a forecast period than are tracker configurations based on individual parameters. Configurations that included both wind- and pressure-based variables outperformed those composed of only one type or the other.

OAR Goals: Make Forecasts Better

Tracker Configurations: Mean of All Parameters Provides Best Guidance



Scatterplots indicating two aspects of forecast track error (FTE) for GFDL vortex tracker configurations based on individual parameters, compared to a configuration based on the mean of all individual parameters. Values along the y-axis indicate the frequency of superior performance of superior (%) as calculated in head-to-head comparisons of FTE for each individual configuration, versus the configuration based on the mean of all 11 parameters. Values less than 50% indicate weaker performance of an individual configuration compared to that of the mean configuration. Values along the x-axis show the relative FTE (%) based on individual parameters compared to the FTE based on the mean of all 11 parameters. Symbols plotted to the left (right) of the vertical dashed line in each panel indicate a configuration with smaller (larger) FTEs than the 11-parameter mean fix.

¹NOAA/Geophysical Fluid Dynamics Laboratory, Princeton, NJ